TRR
JOURNAL OF THE TRANSPORTATION RESEARCH BOARD

Research Article

Transportation Research Record
1–19

DOI: 10.1177/0361198119838270
journals.sagepub.com/home/trr
SAGE

Joint Optimization Scheme for the Planning and Operations of Shared Autonomous Electric Vehicle Fleets Serving Mobility on Demand

Colin J. R. Sheppard[1], Gordon S. Bauer[2], Brian F. Gerke[1], Jeffery B. Greenblatt[3], Alan T. Jenn[4], and Anand R. Gopal[1]

Abstract

As the transportation sector undergoes three major transformations—electrification, shared/on-demand mobility, and automation—there are new challenges to analyzing the impacts of these trends on both the transportation system and the power sector. Most models that analyze the requirements of fleets of shared autonomous electric vehicles (SAEVs) operate at the scale of an urban region, or smaller. A quadratically constrained, quadratic programming problem is formulated, designed to model the requirements of SAEVs at a national scale. The size of the SAEV fleet, the necessary charging infrastructure, the fleet charging schedule, and the dispatch required to serve demand for trips in a region are treated as decision variables. By minimizing both the amortized cost of the fleet and chargers as well as the operational costs of charging, it is possible to explore the coupled interactions between system design and operation. To apply the model at a national scale, key complications about fleet operations are simplified; but a detailed agent-based regional simulation model to parameterize those simplifications is leveraged. Preliminary results are presented, finding that all mobility in the United States (U.S.) currently served by 276 million personally owned vehicles could be served by 12.5 million SAEVs at a cost of $ 0.27/vehicle-mile or $ 0.18/passenger-mile. The energy requirements for this fleet would be 1142 GWh/day (8.5% of 2017 U.S. electricity demand) and the peak charging load 76.7 GW (11% of U.S. power peak). Several model sensitivities are explored, and it is found that sharing is a key factor in the analysis.

The transportation sector represents the fastest-growing segment of the world's greenhouse gas (GHG) emissions, with cars accounting for 8.7% of global energy-related carbon dioxide emissions in 2013, and car sales set to more than double by 2050 (*1*). In 2017, the transportation sector became the largest emitter of greenhouse gases in the United States (U.S.), overtaking emissions from the electric power industry (*2*). Transportation, therefore, represents one of the primary challenges to achieving deep decarbonization of the U.S. economy (*3*, *4*).

Plug-in electric vehicles (PEVs) have emerged as a market-ready technology with the potential to dramatically reduce the carbon intensity of private transportation (*5*, *6*). Prior research has proven the capability of PEVs to meet the travel needs of the majority of drivers in the U.S. (*7*, *8*). Nine U.S. states (California, Connecticut, Maryland, Massachusetts, New Jersey, New York, Oregon, Rhode Island, and Vermont) have established zero-emission vehicle mandates which combined will lead to deployment of 12 million vehicles, mostly PEVs, in the U.S. by 2030 (*9*–*11*).

Simultaneously, other important trends are emerging in the transportation sector. This study attempts to align these trends in a coupled evaluation of electric vehicles with shared autonomous on-demand mobility services. In the remainder of the introduction, future trends in transportation are examined and their potential impact on electrification is discussed. This is followed by an overview of analytical approaches that have been

[1]Lawrence Berkeley National Laboratory, Berkeley, CA
[2]UC Berkeley, Berkeley, CA
[3]Emerging Futures LLC, Berkeley, CA
[4]UC Davis, Davis, CA

Corresponding Author:
Address correspondence to Colin J. R. Sheppard: colin.sheppard@lbl.gov

employed to model PEV usage which are drawn upon for this work.

Future Trends in Transportation

Automation and Shared Mobility. The transportation sector is transforming through the introduction of on-demand mobility and through vehicle automation (*12*). Increased use of smartphone-enabled shared mobility services through transportation network companies (TNCs) such as Uber and Lyft, are already implicated in reductions in private vehicle ownership (*13*). Automation, too, may result in significant changes in how people use vehicles and their associated energy consumption. Self-driving vehicles are already on the roads, serving passengers in the U.S. without a human backup driver in the vehicle (*14*). Synergy among these "three revolutions" could result in deep GHG reductions (*15*, *16*, *17*).

However, adoption of PEVs has been relatively slow for several reasons, including technological uncertainty, slow charging, range anxiety, and higher capital costs compared with other types of vehicle (*18*, *19*). The leading developer of vehicle automation technology, Waymo, has entered an agreement to purchase 20,000 PEVs by 2020 (*20*). While there is still a great deal of uncertainty around the impact that automated vehicles (AVs) will have on the transportation system in the coming decades, there is little doubt that they will soon be a part of the transportation system and could dramatically disrupt conventional modes of mobility (*21*, *22*). There is a wide variety of business models that could make use of AVs (*23*). The success of these business models will depend on their relative cost structures, regulatory burden, consumer acceptance, and a host of other factors (*24–26*). However, there is growing consensus that without sharing rides, that is, more than one passenger per vehicle, the end result of vehicle automation could increase undesirable outcomes like vehicle miles traveled, congestion, energy consumption, and emissions (*16*, *27*, *28*).

Shared automated electric vehicles (SAEVs) could offer on-demand transportation in electric and self-driving cars similar to the service provided by current TNCs but likely at much lower cost and carbon intensity (*29*). Because each SAEV need only have enough seats (known as "right-sizing") and battery range for the trip requested and charging can be split over many short periods in between trips, the shared mobility paradigm could enable the use of smaller cars with shorter battery range, thus overcoming the barriers of slow charging speed and high capital cost (*17*, *30*, *31*).

Furthermore, because shared vehicles typically travel many more miles annually than private vehicles, deployment of SAEVs would increase the per-vehicle GHG reductions relative to private ownership and spread the capital costs over more miles. SAEVs deployed in 2030 could reduce GHG emissions per mile by more than 90% relative to privately owned conventional vehicles while substantially increasing cost-effectiveness (*17*). A recent Rocky Mountain Institute report predicted that the marginal cost of SAEVs could fall below that of conventional private vehicles leading to market dominance by 2050 (*32*). It is possible that such cost savings will increase overall vehicle miles traveled as a result of induced demand, but some studies have predicted that the efficiency gains would outweigh any resulting potential increases in emissions (*12*).

Charging Infrastructure and Vehicle Grid Integration. Public PEV charging infrastructure is a critical component to accelerate the adoption of PEVs (*33–35*). However, there is a weak business case for the private sector to invest in chargers in the context of personally owned PEVs (*36*). Governments across the world have therefore initiated campaigns to support the planning and installation of charging infrastructure to varying degrees (*11, 37–40*).

PEV charging introduces a significant new load to an electric system that is already challenged to meet peak electricity demand multiple times each year, as well as incorporate increasing levels of intermittent wind and solar generation. As intermittent renewable capacity increases, the incidence of renewable energy (RE) curtailment increases which raises the overall system cost of supplying electricity (*41*). In addition, some utilities must meet a renewable energy production standard to satisfy regulatory mandates, so renewable curtailment forces them to either acquire more RE or introduce sources of grid flexibility to relieve the curtailment (*42*).

Many studies have assessed the benefits of coordinated PEV charging on electric power system operations, (*43–45*). If charging is properly coordinated, it can provide a dual benefit of decarbonizing transportation while lowering the capital costs for widespread renewables integration and reducing the need for energy storage (*46–49*). The capability of PEVs to enhance the integration of renewable energy sources, including wind and solar, into the existing power grid has been widely discussed (*50–61*).

Analytical Approaches

PEV models typically fall into two groups: trip-based models and activity-based models. Trip-based models typically summarize or infer travel patterns from travel survey data and use them to characterize the need for PEV charging infrastructure and the temporal opportunities to charge (*62–64*). Such approaches cannot account for the individual mobility constraints of travelers and

they typically require an assumption that charging infrastructure is unlimited.

The most common form of activity-based PEV models make use of travel diaries from surveys or GPS data logging which are then provided as input to energy and charging simulations that estimate the energy consumption and state of charge of the PEV batteries and therefore the necessity or propensity to recharge at the conclusion of trips (*65–68*).

Agent-based models—a subset of activity-based models—treat travelers individually and require a representation of each individual's activity schedule to model the travel necessary to engage in those activities. Several previous studies have employed agent-based modeling techniques to explore the feasibility of a fleet of automated taxis operating in an urban environment (*24*, *29*, *69–74*). Building on these results, Bauer et al. developed an agent-based model to predict the system costs of a fleet of SAEVs operating in New York City (NYC) and design a heuristic process to size the fleet and dispatch the vehicles to serve demand that is derived from trip data or stochastically created (*31*). This model is referred to as the Bauer, Greenblatt, Gerke (BGG) model.

Previous studies have shown that electric taxi fleets are viable options under certain circumstances. However, those studies have chosen fixed values for various fleet parameters. To the authors' knowledge, Bauer et al. was the first study to explore a variety of vehicle, operational, and infrastructure parameters to identify the fleet configuration with lowest cost, and the corresponding environmental and energy impacts (*31*). It also assumed that taxis can relocate to charge whenever they are idle, which may reduce both the required battery range and overall cost as well as the impact of the vehicle fleet on the power grid.

In this work, a hybrid analytical approach is used. A trip-based optimization model is developed that can scale to a national scope and key assumptions and parameters for this trip-based model are developed by applying the BGG model in nine urban regions.

Approach

The primary contribution of this analysis is the optimization model. This model treats the size of the PEV fleet and the amount of charging infrastructure as continuous decision variables (relaxing the problem from mixed-integer to quadratic), allowing for heterogeneous vehicle ranges and charger levels. The model minimizes operational costs by choice of the timing of fleet recharging while requiring that mobility demand be served and energy conserved. Planning costs are simultaneously minimized by amortizing the cost of the fleet and charging infrastructure to a daily time period. For a full model specification, see the section "Model Specification".

In addition to developing the optimization model, a set of empirically derived inputs and assumptions for the model application is also curated. While more work is needed to refine the model and assumptions (see the section "Gaps and Shortcomings"), it is believed that useful insights can already be gleaned from the results of the modeling workflow. These are discussed in detail in the section "Results and Discussion".

Figure 1 illustrates the source of all major model inputs and assumptions including intermediate modeling and analysis used in their derivation. Each model input is described in further detail below, beginning with the specification of the optimization model.

Model Specification

The dimensions of the model include time t, region r, vehicle battery size b, charger level l, and trip distance d. The model is quadratic in the objective as well as the constraints and therefore can be efficiently solved with a second-order cone programming solver.

Objective. The objective is to minimize the amortized daily cost of the fleet, the infrastructure, and the fleet operations.

$$\min Z = \sum_r \left(\sum_t C_{tr} + I_r^c + I_r^V \right) \tag{1}$$

where C_t is the operations cost in hour t and region r, I_r^c is the amortized daily charging infrastructure cost, and I_r^v is the amortized daily fleet cost.

Constraints. **Operations Cost**: cost of electricity energy and capacity, as well as mileage-dependent vehicle maintenance.

$$C_{tr} = \sum_b \left(\sum_l P_{btlr} \tau_{tr} + \beta_v \sum_d \rho_d D_{bdtr} \right) + P_r^{max} \beta_r / N_T \tag{2}$$

where P_{btlr} is the energy dispensed for charging by vehicle class b in time t using level l in region r, τ_{tr} is electricity price (\$ / kWh), β_v is the per-mile vehicle maintenance cost, ρ_d is the average travel distance in miles per passenger trip for distance bin d, D_{bdtr} is the allocated demand for trips, P_r^{max} is the maximum power demanded over the time horizon, β_r is the average demand charge for the region (\$/kW/day), and N_T is the number of time steps in the simulation (this turns the demand charge, which is

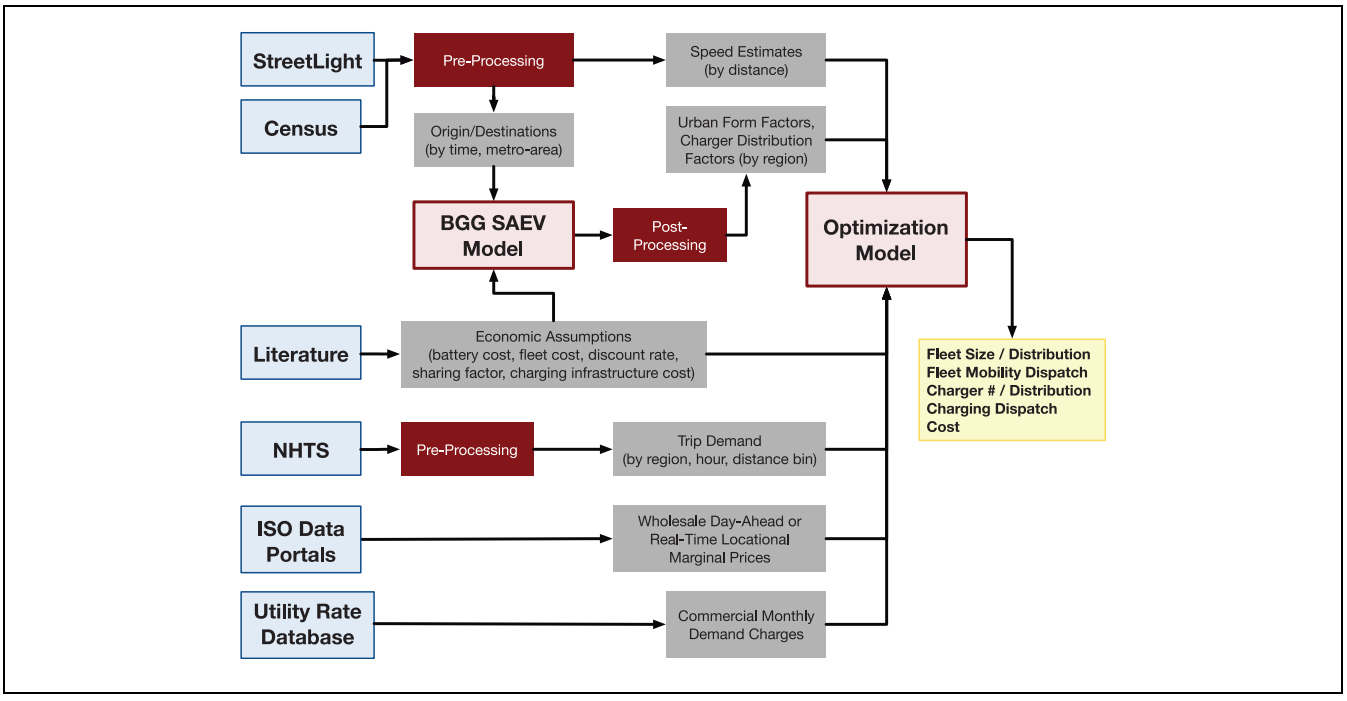

Figure 1. Sources of data (*blue*), data processing (*dark red*), models (*light red*), intermediate data (*grey*), and model outputs (*yellow*) in the overall modeling and processing workflow.

levied once per day, into an hourly cost). In reality, demand chargers are usually levied on a monthly basis, so this daily charge neglects the fact that day to day variation would likely lead to a higher monthly payment than a simulation based on a single day. This can be compensated for through sensitivity analysis or increasing the number of simulated days; a task for future work.

Infrastructure Cost: in this constraint, the charger distribution factor accounts for spatial mismatch between vehicle locations and available charger locations as well as overbuilding necessary to decentralize chargers. In other words, for a given number of vehicles charging, additional charging infrastructure is required, assuming that not all chargers are sited in the right location at the right time.

$$I_r^c = \sum_l N_{lr} \gamma_l \delta_l \theta_l^c \tag{3}$$

where δ_l is the charger distribution factor, γ_l is the power capacity of the charger (kW), and θ_l^c is the amortized daily charger cost ($/kW):

$$\theta_l^c = \frac{\phi_l^c r(1+r)^{L^c}}{(1+r)^{L^c} - 1} \tag{4}$$

where ϕ_l^c is the capital cost of charger of level l, L^c is the lifetime of the charger in days, and r is the daily discount rate.

Fleet Cost: in this constraint, battery costs are considered separately from the rest of the vehicle.

$$I_r^V = \sum_b V_{br}^* (\theta^v + \theta^b B_b) \tag{5}$$

where V_{br}^* is the fleet size, θ^v is the amortized daily vehicle cost (without a battery), θ^b is the amortized daily battery cost ($/kWh), B_b is the battery capacity (kWh).

$$\theta^v = \phi_{om}^v + \frac{\phi^v r(1+r)^{L^v}}{(1+r)^{L^v} - 1} \tag{6}$$

$$\theta^b = \frac{\phi^b r(1+r)^{L^b}}{(1+r)^{L^b} - 1} \tag{7}$$

where ϕ_{om}^v is the daily variable operations and maintenance (O&M) cost for the vehicle, ϕ^v is the capital cost of the vehicle, and L^v is the lifetime of the vehicle in days. And where ϕ^b is the capital cost of the battery ($/kWh), and L^b is the lifetime of the battery in days.

Energy to Meet Demand: the energy consumed by the fleet is a function of the number of trips served, the conversion efficiency of the vehicles, the urban form (which determines the length of empty vehicle trips), and ride sharing. The effect of urban form and sharing are modeled as multipliers on the energy efficacy of serving mobility demand.

$$E_{bdtr} = \frac{D_{bdtr}\mu_r\eta_b\rho_d}{\sigma_d} \quad (8)$$

where E_{bdtr} is the energy consumed serving mobility of vehicle type b and trip length d in hour t and region r, σ_d is the sharing factor or the average number of passengers per vehicle trip, μ_r is the urban form factor or one plus the ratio of empty vehicles miles driven to vehicle miles driven with passengers, and η_b is the conversion efficiency of the vehicle power train (kWh/mile).

Vehicles Moving: the number of vehicles actively serving trips is related to trip demand and the sharing factor. The term $\frac{\rho_d}{\Delta t \nu_{dt}}$ corrects for the length of the time period, allowing, for example, one vehicle to serve two trips in an hour if the distance to speed ratio is 1/2.

$$V^m_{bdtr} = \frac{D_{bdtr}\rho_d}{\sigma_d \Delta t \nu_{dtr}} \quad (9)$$

where V^m_{bdtr} is the number of vehicles of type b serving mobility demand of trip length d in hour t and region r, ν_{dtr} is the average velocity of vehicles, and Δt is the length of the time period in hours.

Vehicles Charging: the number of vehicles charging is related to the power consumed by the capacity of each charger type.

$$V^c_{btlr} = \frac{P_{btlr}}{\gamma_l} \quad (10)$$

where V^c_t are the number of vehicles charging in hour t, and γ_l is the charging rate (kW / charger).

Charging Upper Bound: it is assumed that the batteries in fleet start full and therefore can only be replenished up to the cumulative amount consumed by the previous hour.

$$\sum_{\hat{t}=0}^{t}\sum_{l} P_{b\hat{t}lr} \leqslant \sum_{\hat{t}=0}^{t-1}\sum_{d} E_{bd\hat{t}r}, \forall btr \quad (11)$$

Charging Lower Bound: charging must keep up with consumption as limited by the capacity of the batteries. Energy must be supplied by charging in the previous hour to be used in the next hour. This constraint prevents the aggregate state of charge of the vehicles from becoming negative. By constraining only the aggregate state of charge and not constraining individual vehicle states of charge, it is assumed that the fleet can be managed to maintain all individual vehicles appropriately. In practice there could be solutions to the aggregate problem that are challenging to satisfy with the individual vehicles.

$$\sum_{\hat{t}=0}^{t-1}\sum_{l} P_{b\hat{t}lr} \geqslant \sum_{\hat{t}=0}^{t}\sum_{d} E_{bd\hat{t}r} - V^*_{br}B_b, \forall btr \quad (12)$$

No Charge at Start: the first hour of the day needs to have no charging to allow for the convention that charging can only occur after some energy is consumed by the fleet.

$$P_{btlr} = 0, t = 0, \forall blr \quad (13)$$

Terminal State of Charge: the aggregate state of charge of batteries must again be full at the end of the day. This constraint would be too restrictive if the end of the day is defined as midnight (since there is still a fair amount of vehicle miles traveled [VMT] during that hour). The day boundary is therefore shifted to the lowest VMT level of the day, which typically occurs at 4 a.m.

$$\sum_t\sum_l P_{btlr} = \sum_t\sum_d E_{bdtr}, \forall br \quad (14)$$

Demand Allocation: demand must be served by some composition of vehicles.

$$\sum_b D_{bdtr} = DD_{dtr} \quad (15)$$

where DD_{dtr} is exogenous demand in hour t (person trips).

Fleet Dispatch: together vehicles serving trips, charging, and idle cannot exceed the fleet size.

$$\sum_d V^m_{bdtr} + V^i_{btr} + \sum_l V^c_{btlr} \leqslant V^*_{br} \quad (16)$$

Max Charging: vehicles charging cannot exceed the number of chargers.

$$\sum_{bd} V^c_{bdtl} \leqslant N_{lr} \quad (17)$$

where N_{lr} is the number of chargers charging at power level l in region r.

Max Demand: this constraint relates the maximum power consumed for each region to the power drawn in each time period. Because P^{max}_r is in the objective function, there will be no slack in the optimal solution, ensuring it will be equal to the maximum power demanded by the fleet.

$$P^{max}_r \geqslant \frac{\sum_{bl} P_{tblr}}{\Delta t}, \forall tr \quad (18)$$

National Household Transportation Survey (NHTS) Data

The model was applied at a national level based on estimates of hourly demand for private vehicle trips on a typical day, as derived from the 2017 NHTS (*75*). NHTS respondents log trip distance, timing, and vehicle type for

all household members on a specified day. The responses are weighted according to demographics to yield a typical mobility profile over a single day across the U.S.

To produce the trip-demand model inputs, the country is partitioned into 13 broad geographic regions, made up of the nine U.S. Census Divisions, (New England [NE], Mid-Atlantic [MAT], South Atlantic [SAT], East-North-Central [ENC], West-North-Central [WNC], East-South-Central [ESC], West-South-Central [WSC], Mountain [MTN] and Pacific [PAC]) with the four largest states (California, Florida, New York, and Texas) separated out into their own individual regions. We use "NL" to refer to the remainder of the divisions containing the large states, "NL" stands for "Not Large". Hereafter, these regions are referred to interchangeably as "regions" or as the Census-Division-Large-State (CDLS) subdivision. In addition, the trips are subdivided according to an NHTS data field that specifies whether a given respondent is in an urban or a rural area. This yields a total of 26 regional data sets (13 CDLS regions, each with urban and rural subregions). Within each region, all trips are taken in private vehicles (specifically, the following NHTS vehicle type codes: car, SUV, van, pickup truck, motorcycle, RV, and rental car), and weighted counts are computed in eight bins of trip distance, mileage intervals specified by $(0, 2]$, $(2, 5]$, $(5, 10]$,$(10, 20]$, $(20, 30]$, $(30, 50]$, $(50, 100]$, and $(100 - 300]$, with counts computed independently for typical weekdays and weekend days. This specifies the distribution of total daily trip demand by trip distance within each region.

To investigate the dynamics of vehicle charging and the related effects on the grid, it is also necessary to estimate the time variation of trip demand throughout the day. One straightforward approach would be to further subdivide the regional and distance bins by hour to produce hourly distributions of trip demand by distance. However, the NHTS dataset is insufficiently large to support this level of granularity without introducing substantial noise into the trip demand estimates, especially for longer trips and less populous regions. To circumvent this issue, hourly trip distributions (by the hour in which the trip initiated) are separately computed for each distance bin, subdivided by urban vs. rural and weekday vs. weekend, but are aggregated up to the entire U.S., rather than subdivided by CDLS. These hourly trip distributions are then applied to the total trip counts computed within the more granular CDLS regions to produce estimates of the hourly trip volume by distance within each region. The resulting hourly trip distributions thus capture geographical variations in overall trip volume at the detailed CDLS level, while assuming regional differences in the hourly profile of trip demand are insignificant (indeed, disaggregating this calculation into the four U.S. census regions showed regional differences that were noisy but consistent). Figure 2 shows the resulting trip distributions.

StreetLight Data

To determine realistic values for urban form factor and charger distribution factor for the optimization model, trip data obtained from StreetLight Data is coupled with the BGG model. StreetLight Data is a company that aggregates data from cell phones and GPS devices to produce transportation metrics such as travel times and volumes.

First, shapefiles were obtained from the Census Bureau website with census tracts for a series of combined statistical areas, as shown in Table 1. These shapefiles were then uploaded to the StreetLight Data portal, and two types of data were obtained. "Trip attributes" files contained distances, times, and speeds between each pair of census tracts. Data was only provided for zone pairs with a significant number of trips, as determined by StreetLight Data. "Trip Counts" data contained the volume of trips between each census tract origin and every traffic analysis zone (TAZ) with a significant volume, again as determined by StreetLight. The data also contained significant trip counts between each origin TAZ and destination census tract.

Since Streetlight trip attributes were binned into larger intervals (e.g., percent trips with durations between 10 and 20 min, or 5 and 10 mi), the first processing step was to interpolate distributions with increased resolution, binning distributions by 1 min, 0.1 mi, and 1 mph for trip duration, distance, and speed, respectively. To interpolate missing values, the average distributions were found from the three nearest zones, along with data from the nearest zones in the hour before and after. This process was repeated iteratively until over 99% of all O-D pairs had data in all hours for all three attributes.

While this interpolation process introduces a source of error into the model, it is considered acceptable for two reasons: All trip data between census tracts comes from zone pairs with actual data, and in previous work by Bauer et al., it was found that modifying trip relocation times by distributions with mean zero did not significantly change the results (*31*).

Trip counts were binned by hour, so the data was interpolated to estimate the number of trips starting in each minute. Trips starting outside of the combined statistical area (CSA) were removed to avoid double-counting trips between regions.

These pre-processing steps resulted in trip counts for each origin–destination pair by minute, and distributions of duration, distance, and speed for each origin–destination pair by hour. This data was used as input for the BGG model.

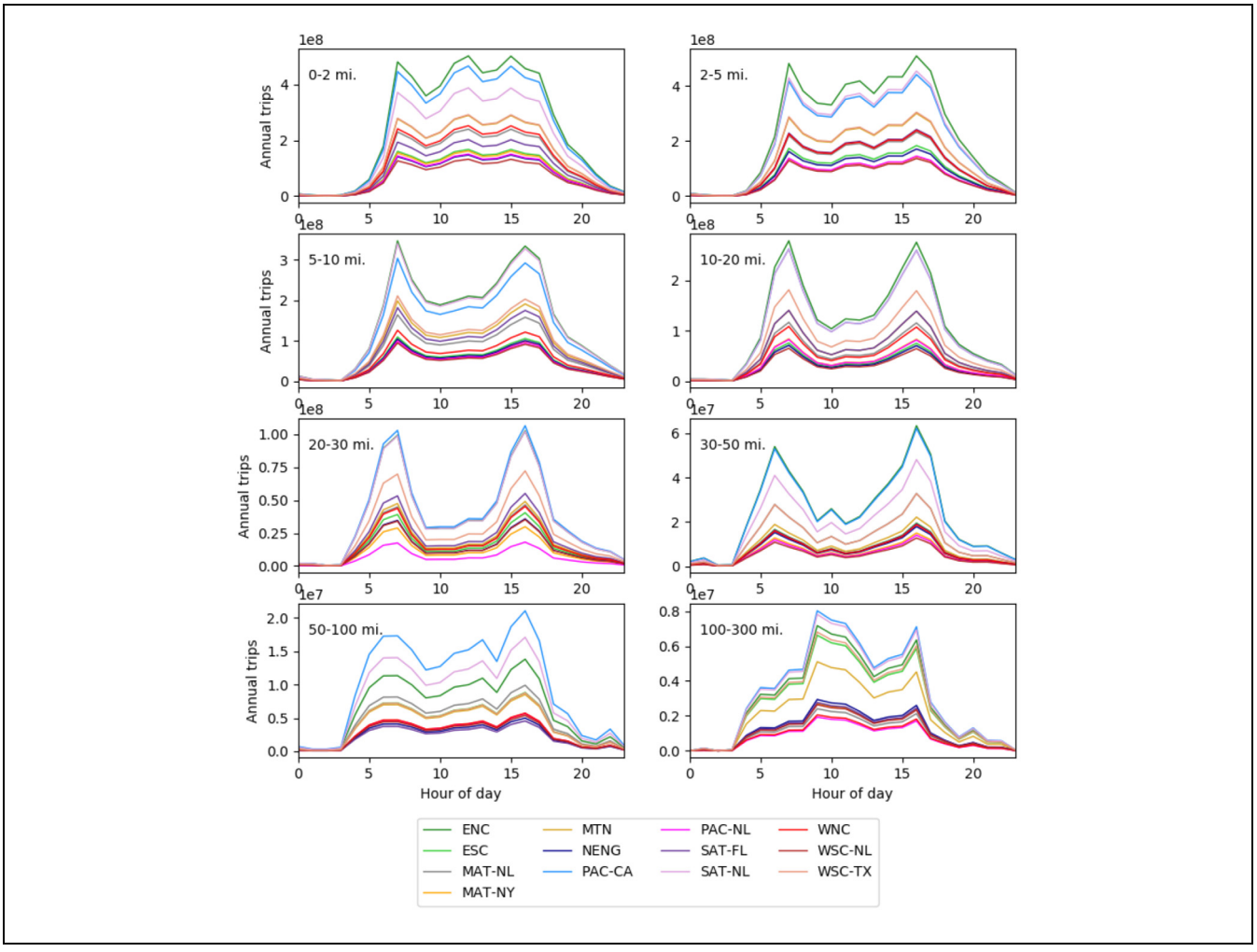

Figure 2. Hourly trip distributions (by hour of trip initation), for weekdays, in bins of trip distance, as estimated from the 2017 NHTS for urban areas in 13 CDLS geographic regions.

The BGG model proceeds chronologically over one day of data, repeating until the fleet's aggregate battery capacity at the end of the day is within 5% of that at the beginning of the day. In each minute, trips are assigned to the nearest vehicle, and idle vehicles are routed to charge or rebalanced in anticipation of future demand (*31*). Travel times and distances between each taxi and trip or charging point are imputed by drawing random values from the corresponding distribution obtained from StreetLight Data. To ensure a reasonable relationship between time, distance, and speed for each trip, distances are re-sorted to best match the relationship between draws for duration and speed. If a trip can only be served by a vehicle with insufficient battery capacity, the vehicle's range is increased by 50-mi increments until capacity is adequate. If no vehicle can serve a trip within a 10-min wait time, a new vehicle is added to the fleet. Thus, both battery range and fleet size increase organically over the course of the simulation, providing estimates of the minimum values required to serve demand.

Simulations were conducted for each city with 100k, 200k, 400k, and 800k trips, and with both 15kW and 50kW charging power. Locations of chargers were determined by k-means clustering of trip origins and destinations, which was determined to work as effectively as the siting algorithm described in Bauer et al. (*31*). Simulations were then run with sufficient chargers to recharge the fleet assuming 25% empty miles and 50% charger utilization, then again, assuming 100% charger utilization. In each case, every charger was occupied during peak charging times, so it was concluded that a charger distribution factor δ_l of 1 would be sufficient.

While the simulation ran, the empty distance traveled for each trip and charging event was recorded, and was aggregated across census tracts to determine the urban

Table 1. Combined Statistical Areas Used for Multi-City Simulations with the BGG Model

Name	Area (1000 km^2)	Census division	Population (1000s)
Buffalo-Cheektowaga, NY	7.4	New York	1214
Charleston-Huntington-Ashland, WV-OH-KY	13.8	South Atlantic	680
Dallas-Fort Worth, TX-OK	42.7	Texas	7846
Fort Wayne-Huntington-Auburn, IN	8.2	East North Central	631
Lafayette-West Lafayette-Frankfort, IN	4.4	West South Central	252
Martin-Union City, TN-KY	3.4	East South Central	70
Rockford-Freeport-Rochelle, IL	5.5	East North Central	434
Seattle-Tacoma, WA	31.8	Pacific	4765
Virginia Beach-Norfolk, VA-NC	10.8	South Atlantic	1829

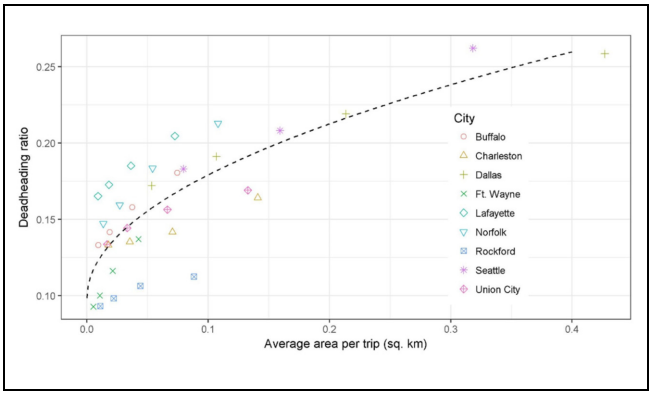

Figure 3. Ratio of empty miles to passenger miles in each simulated CSA versus the ratio of CSA land area to number of trips, with square-root regression line.

form factor μ_r in both rural and urban areas of each city. Following the definition used by NHTS, rural areas were considered to be all census tracts within a CSA not contained within an urbanized area or urban cluster, as determined by the Census Bureau. As shown in Figure 3, it was found that urban form factor increases roughly with the square root of area per trip. Using ordinary least squares regression techniques, these ratios were extrapolated to all other CSAs and urbanized areas in the country based on population and area. Finally, population-weighted means were taken to extrapolate from cities to determine the urban form factor for each census division.

Power Sector Data

To model the fleet operations with reasonable electricity cost estimates, different pricing scenarios were developed that vary over a range of potential economic conditions on the grid. Real time locational marginal price data (or, if unavailable, day ahead price data) was downloaded from five Independent System Operators (ISOs) across the U.S. The ISOs were CAISO, NYISO, PJM, ERCOT, and MISO. Data were downloaded for the entire year of 2017 as well as the first half of 2018. Across all five ISOs and all locational pricing nodes, the median price from each hour of the day was taken across the entire data set. In addition, median prices were taken for each combination of ISO and month and some of the resulting price profiles were used in one sensitivity analysis (see section "Price Shape"). The average of the price profiles was then subtracted and \$ 0.09/kWh was added to produce a price shape that keeps the hourly variation in price from the wholesale sector, but has an average daily price equivalent to the average commercial retail electricity rate in the U.S. as estimated by the Energy Information Agency (*76*). This hybrid approach allows the overall cost to reflect the end-user cost of purchasing electricity while also allowing the fleet to take advantage of price arbitrage opportunities throughout the day. The loads from these fleets will be very large in aggregate, so it is reasonable to expect they will somehow be able to participate in wholesale power markets.

The final price assumption for the base scenario is shown in Figure 4 along with 4 other pricing scenarios. The "CAISO-Duck" scenario is based on the California median price of electricity in March, 2017; the "ERCOT-Summer" scenario is based on Texas prices in July, 2018, and the "NYISO-Winter" scenario is based on New York in January, 2018.

Based on data from the Utility Rate Database, a median national retail rate for demand charges in the U.S. was estimated (*77*). The data was subsetted to commercial rate schedules and then the demand charge price from the primary monthly period was taken (i.e., if multiple time-of-use periods are defined, only the first period in the database was used) and the median was found to be \$7.7/kW/month. The interquartile range was from \$3 to \$10.7, demonstrating substantial variability in prices nationwide. It was found however, that model results are largely insensitive to this assumption.

Key Assumptions

Table 2 lists all key assumptions used for the Base scenario of the optimization model.

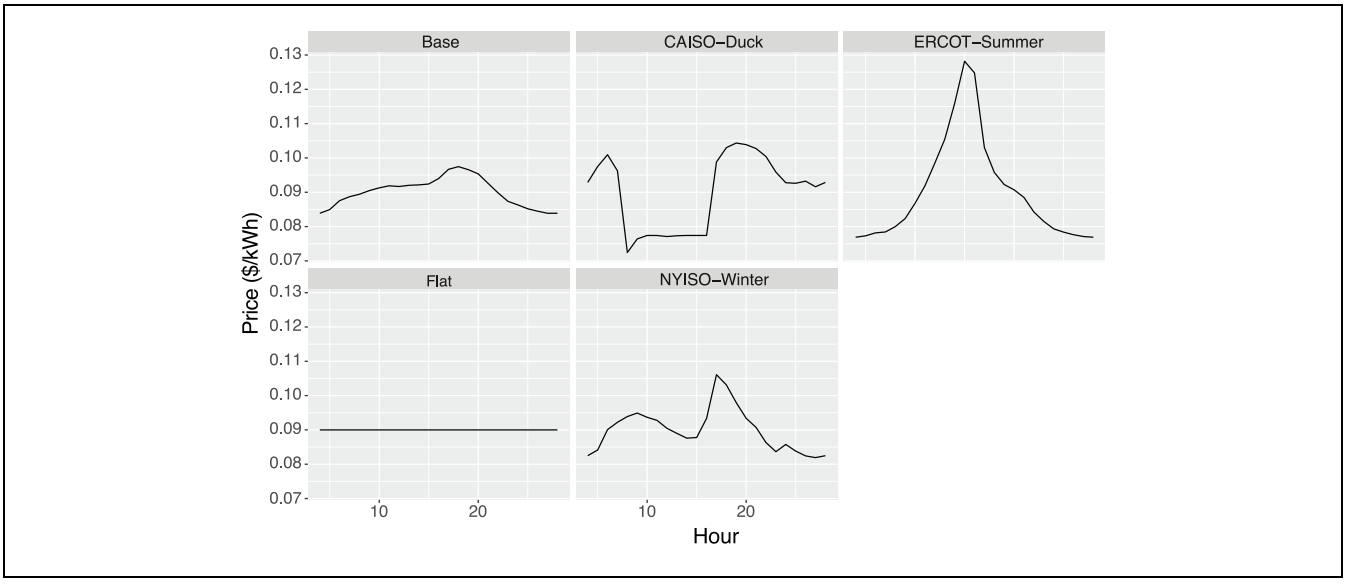

Figure 4. Diurnal electricity price used in price shape experiment. Shapes are derived from 2017–2018 wholesale marginal pricing data from various ISOs. Each profile has an average price of $ 0.09/kWh.

Table 2. Key Modeling Assumptions Used to Define the Base Scenario

Input	Symbol	Value(s)
Charger types and power	γ_l	L010=10kW, L020=20kW, L050=50kW, L100=100kW, L250=250kW
Charger capital cost	ϕ_l^c	L010=$5k, L020=$11k, L050=$35k, L100=$95k, L250=$425k
Charger lifetime	L^c	10 years
Charger distribution factor	δ_l	1.0 for all types
Demand charge price	β_r	$7.7/kW/month
Energy price	τ_{tr}	See Figure 4
Annual discount rate	r	0.05
Number of distance bins	$Card(d)$	10
Urban form factor	μ_r	See Figure 10
Sharing factor	σ_d	1.5
Vehicle capital cost	ϕ^v	$30,000 (includes cost of automation)
Vehicle daily fixed O&M	ϕ_{om}^v	$ 0.64
Vehicle per-mile O&M	β_v	$ 0.09
Battery capital cost	ϕ^b	$150/kWh
Vehicle/battery lifetime	L^v,L^b	3.4 years
Battery capacity	B_b	75mi range=19.7kWh, 150mi range=41.1kWh, 225mi range=64.4kWh, 300mi range=89.4kWh, 400mi range=124.0kWh
Conversion efficiency	η_b	75mi range=0.262kWh/mi 150mi range=0.274kWh/mi 225mi range=0.286kWh/mi 300mi range=0.298kWh/mi 400mi range=0.310kWh/mi
Speed by distance bins	ν_{dtr}	1.1 to 3.6mi = 18mph, 13.4 to 14.1mi = 32mph 24.1mi = 38mph, 35.5mi = 40mph 60.3 to 69.6mi = 45mph, 159.9mi = 48mph

Table 3. Optimal System Configuration and Operational Statistics for the Base Scenario

Division	Region type	Demand (GWh/day)	Peak (GW)	VMT ($\times 10^6$)	Fleet ($\times 10^3$)	Chargers ($\times 10^3$)	L010 ($\times 10^3$)	L020 ($\times 10^3$)	L050 ($\times 10^3$)	L100 ($\times 10^3$)	% of US demand	% of US peak	Cost ($/mi)
National	All	1142	76.7	3012	12,529	2401	599	680	1102	19	8.5	11	0.266
ENC	Rural	67.2	4.64	176	599	166	91	0	74	0	0.5	0.69	0.246
ENC	Urban	109	7.16	291	1275	232	29	109	93	0	0.81	1.1	0.271
ESC	Rural	43.3	3.05	116	366	99	53	0	40	4	0.32	0.45	0.238
ESC	Urban	45.3	2.99	172	499	86	7	33	44	0	0.34	0.44	0.211
MAT-NL	Rural	15.7	1.1	28	140	41	24	0	17	0	0.12	0.16	0.319
MAT-NL	Urban	51.2	3.33	135	593	106	13	49	44	0	0.38	0.49	0.271
MAT-NY	Rural	12.4	0.868	30	120	30	16	0	14	0	0.092	0.13	0.262
MAT-NY	Urban	34.1	2.26	78	407	69	7	30	31	0	0.25	0.34	0.302
MTN	Rural	20.6	1.41	49	172	40	21	0	13	5	0.15	0.21	0.254
MTN	Urban	57.2	3.86	168	753	131	29	50	51	0	0.43	0.57	0.267
NENG	Rural	17.8	1.23	32	164	38	17	0	21	0	0.13	0.18	0.321
NENG	Urban	30.7	2	58	371	72	14	35	23	0	0.23	0.3	0.347
PAC-CA	Rural	10.9	0.723	24	79	17	5	0	10	1	0.081	0.11	0.249
PAC-CA	Urban	119	7.76	360	1362	227	10	106	110	0	0.89	1.2	0.247
PAC-NL	Rural	10.5	0.722	28	79	23	12	0	9	1	0.078	0.11	0.227
PAC-NL	Urban	29.8	1.98	81	347	57	4	23	29	0	0.22	0.29	0.266
SAT-FL	Rural	6.92	0.485	21	69	13	4	0	8	0	0.052	0.072	0.233
SAT-FL	Urban	56.2	3.81	93	736	110	6	47	55	0	0.42	0.57	0.403
SAT-NL	Rural	64.7	4.56	140	570	162	94	0	63	4	0.48	0.68	0.277
SAT-NL	Urban	110	7.33	300	1277	209	26	68	113	0	0.82	1.1	0.266
WNC	Rural	35.6	2.39	103	294	78	38	0	40	0	0.27	0.36	0.224
WNC	Urban	42.6	2.85	105	570	95	20	37	38	0	0.32	0.42	0.304
WSC-NL	Rural	19	1.2	45	178	26	0	4	22	0	0.14	0.18	0.267
WSC-NL	Urban	27.3	1.78	81	350	57	2	34	21	0	0.2	0.26	0.262
WSC-TX	Rural	26.5	1.82	62	210	56	28	0	25	2	0.2	0.27	0.251
WSC-TX	Urban	78.8	5.33	225	938	150	18	48	83	0	0.59	0.79	0.260

Note: VMT = vehicle miles traveled.

Gaps and Shortcomings

There are several gaps in the model specification and assumptions that should be kept in mind when considering model results. In future research many of these shortcomings will be addressed.

- This model is only concerned with the distant hypothetical future where SAEVs are a dominant mode of transportation. In future work, personally owned electric vehicles and their respective impact on vehicle grid interactions will be added to the model to analyze the transition to such a future.
- Price is exogenously defined. In reality, the load and charging flexibility of an SAEV fleet would be enough to influence the cost of generating power. In future work, power production costs will be made endogenous to the model.
- Mobility demand is exogenously defined. In reality, demand for mobility responds to the cost, travel time, and convenience of the transportation alternative both when competing against other modes but also with respect to long term shifts in land use and travel patterns. In future work, the demand assumptions will be more closely aligned with detailed regionally travel demand analyses that do account for these feedbacks.
- The time used across all of the regions is in local time. While this should not impact the dynamics of fleet dispatch to serve mobility, the resulting charging profiles are inappropriately assumed to be additive by hour.
- The mobility assumptions only cover a typical weekday; a more accurate planning model would include weekend/holiday in the model and weight the operational costs of these days to produce an annualized cost.
- The speed distributions are exogenous and fixed, the impact of congestion on travel times is therefore being ignored. This is a major feedback that can only be addressed through more extensive use of detailed travel demand models that simulate traffic flow.
- Electricity price is based on a median price and the simulation only runs for one day. Electricity prices are highly variable by day and season. An improved model would include multiple days in the simulation representative of a full year.
- The model does not consider temporal overheads associated with charging (e.g., maneuvering to spot, plugging in, etc.) and with maintenance (e.g., cleaning the vehicle interior). These processes could be approximated by derating the charging power associated with each charger level.
- The model ignores the impact of C-rate and battery degradation on system cost and performance. In particular, the fact is ignored that, in high power charging, the charging rate must be reduced past a vehicle state of charge of 80% before charging can commence.
- The model ignores the difference in battery lifetime among vehicles with different-sized batteries. These would not age at the same rate, and should therefore be disaggregated.
- The model does not attempt to optimize the seating capacity of the vehicles.
- We neglect medium/heavy duty vehicle electrification that will likely take place along with passenger vehicle PEVs and have impacts on aggregate electricity consumption and peak load.
- We assume a constant sharing factor across the model, but it likely varies by region, trip distance, and time of day.
- We estimate the variability of urban form factor by region, but it likely also varies by trip distance and time of day.
- We neglect the cost of parking. This is due primarily to the challenge of estimating regional average parking costs in addition to the fact that under a high penetration SAEVs, parking would become much less limited in general, making current parking prices unrepresentative of future costs.

Results and Discussion

In light of the gaps described above, the preliminary results of running the model for the entire U.S. are presented. These results should be interpreted as generally indicative of the characteristics of a national SAEV fleet, not as a high-confidence prediction.

Base Scenario

We present high-level summary metrics for the cost minimizing configuration of vehicle fleet, charging infrastructure, and charging profiles resulting from the Base scenario in Table 3 at both the national and regional scales.

If all U.S. mobility was satisfied by SAEVs with a sharing factor of 1.5, a fleet of only 12.5 million vehicles and 2.4 million charge points would be required, consuming 1,142 GWh of energy per day (or 8.5% of daily U.S. electricity demand) with a peak load of 76.7 GW (or 11% of the U.S. non-coincident peak) at a cost of $ 0.27/mi. The distribution of power capacities in the charging infrastructure is strongly weighted toward 50kW chargers (Table 3), but the solution includes

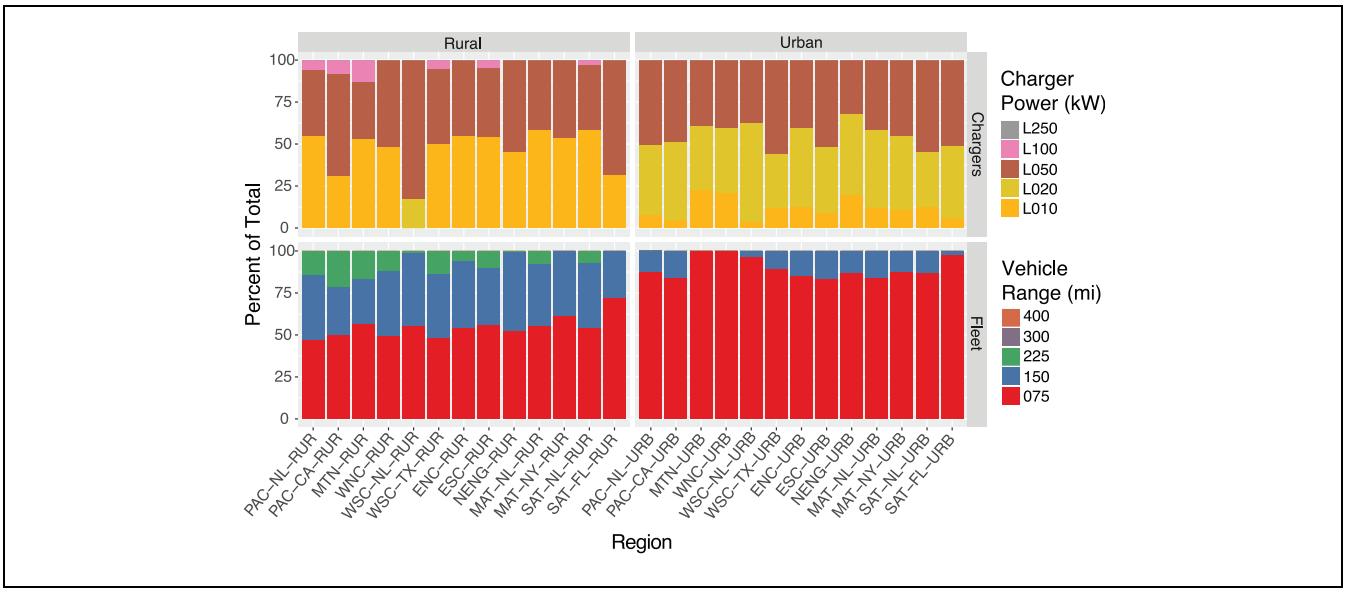

Figure 5. Optimal distribution of fleet vehicles and charging infrastructure for base scenario.

substantial numbers of lower power chargers as well, roughly split between 10kW and 20kW chargers.

The regionally disaggregated results tend to follow predictable patterns that are closely related to the population of the region, and therefore demand for mobility. When comparing demand for charging in specific regions with current-day electricity demand, the result can be quite different from the national average. For example, the 2017 peak load in CA is 50GW and the simulated charging peak is 6.5GW, or 17% of the current peak. This represents a large increase in load and the management of the fleet charging would be of major consequence to the grid operator.

The distribution of vehicle types and charger power by region are shown in Figure 5. There are clear, systematic differences in fleet composition between urban and rural sub-regions, with a greater reliance on longer-range vehicles in the rural areas where trip lengths are longer (12.4 mi on average versus 7.8 for urban). The charging infrastructure requirements in rural regions often include 100kW chargers while the urban regions can be satisfied by lower-power chargers.

In Figure 6, the bulk dispatch of the vehicle fleet between moving, charging, and sitting idle is shown over the course of the day. The total size of the fleet is determined by the afternoon peak for mobility demand (4 p.m. rush hour). Despite the steep drop in demand for mobility into the evening hours, overnight charging of the fleet doesn't begin until after midnight (hour 25) taking advantage of the steadily decreasing marginal electricity price (Figure 4).

In Figure 7, the daily profile of aggregate energy stored in the batteries of the fleet is shown, disaggregated

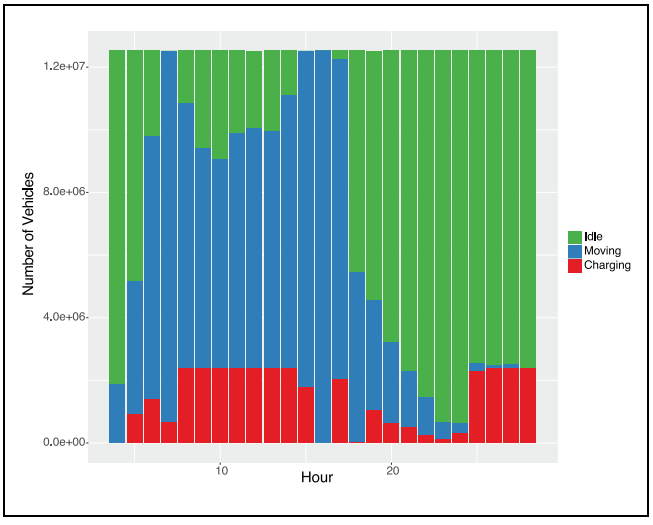

Figure 6. Vehicle dispatch by hour between moving (i.e., serving mobility demand), charging, or sitting idle.

by vehicle type. The batteries are assumed to start the day full and this energy is used to meet the morning rush hour with some modest recharging in the early hours of the day. After the 7 a.m. mobility peak, roughly half of the fleet that is not needed for serving mobility is continuously recharged until the afternoon rush begins at 3 to 4 p.m. This charging replenishes the energy in the fleet sufficiently to allow mobility to be served through the afternoon rush into the late evening with very little charging. It is acknowledged that the aggregate state of charge depletes almost to zero which is unlikely to be acceptable to fleet managers. In future analysis, this lower bound

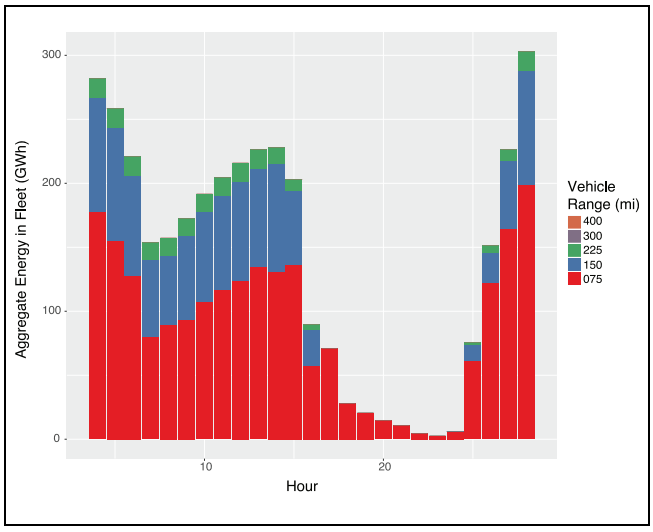

Figure 7. Aggregate energy stored in national fleet batteries by vehicle range by hour of day.

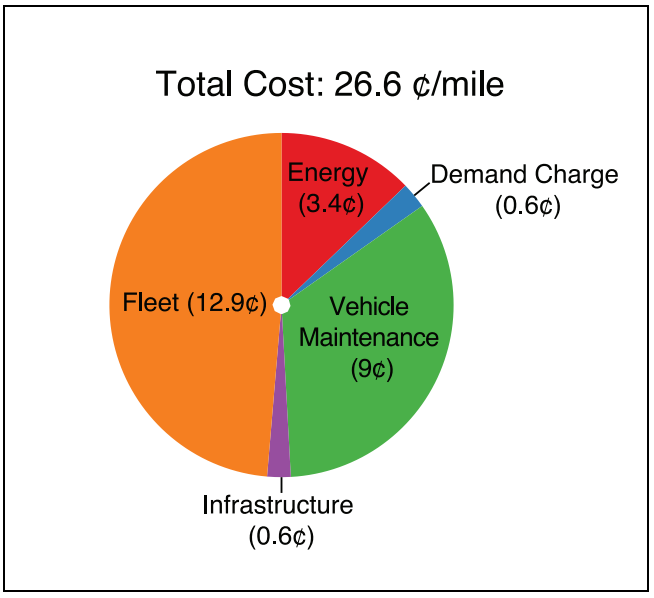

Figure 9. Cost per mile by cost category for the base scenario.

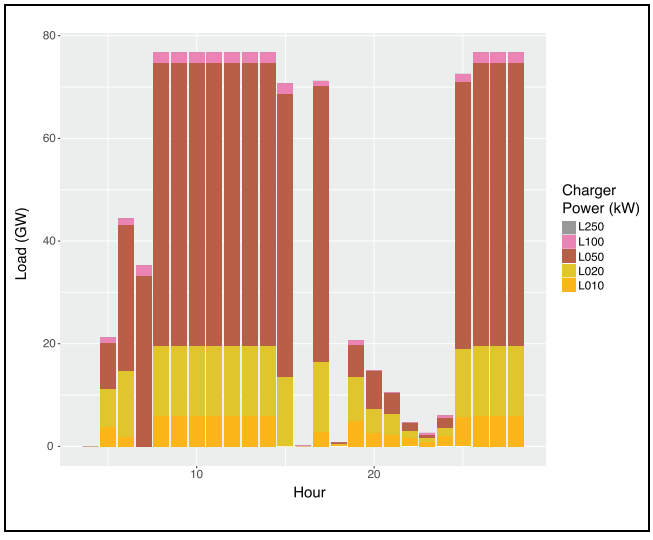

Figure 8. Charging profile of national fleet by charger power capacity.

will be constrained to allow for energy reserves and operational flexibility.

Finally, Figure 8 shows the distribution of charging by charger power capacity over the course of the day. During peak charging hours, all chargers are in use. During most of the rest of the day, the distribution of charging is roughly proportional to the charging infrastructure distribution.

Also of note in the regional results is that the per-mile cost does not vary in a consistent manner between urban vs. rural regions. Vehicle cost is the largest contributor to overall cost (Figure 9). The variation in urban vs. rural regions is therefore largely driven by the composition of the fleet, which ultimately is a result of the particular distribution of mobility demand for each region. Based on a regression analysis, 45% of the variation in the difference in cost between urban and rural regions can be explained by the relative differences in the demand for person trips and for person miles traveled in the regions. The differences in urban form factor between urban and rural regions (Figure 10) were not predictive of the cost results. The other potential explanations for the variation include the timing of mobility, an effect that will be explored in future research.

Illustrative Sensitivities

We conducted several sensitivity experiments to assess the response of the optimal solution to key model inputs and assumptions.

Ride Sharing. The first analysis involves varying the assumption of ride sharing, as this is a parameter that is widely recognized to have a dramatic impact on system outcomes. In Figure 11, the fleet and charger composition are shown for each scenario in the experiment. Because the sharing factor is a simple multiplier on demand, the optimal solution is identical in all respects except that many decision variables are simply scaled. Across all metrics of interest (fleet size, charger requirements, electricity demand, etc.) the solution is scaled in proportion to the sharing factor.

While these results are uncomplicated, they do highlight the power of sharing in a future transportation system. It has immense potential to improve the efficiency

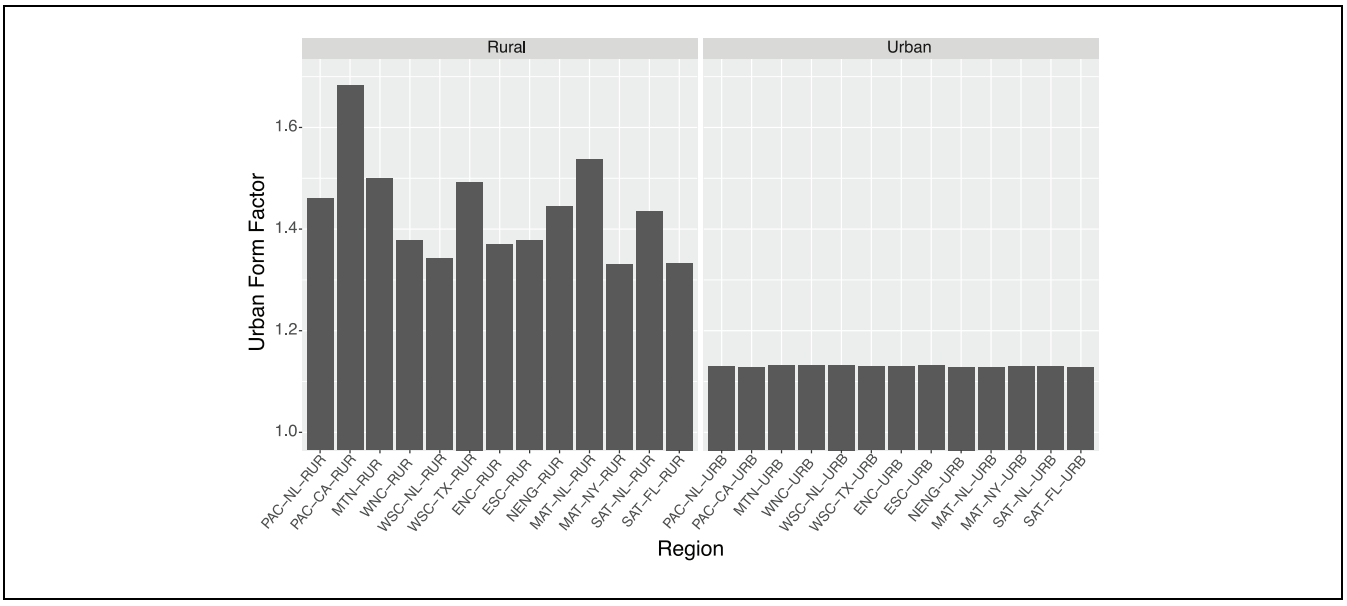

Figure 10. Urban form factor (μ_r) for each region in the base scenario.

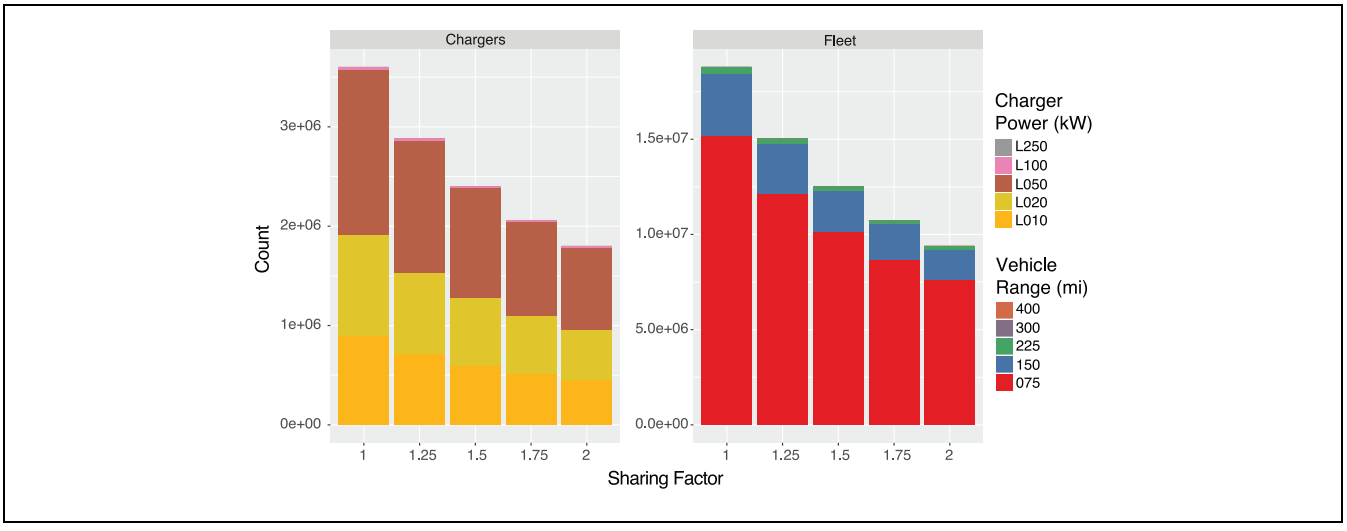

Figure 11. National charging infrastructure (*left*) and fleet composition (*right*) requirements for varying assumptions on sharing factor σ_d (*x*-axis).

of mobility and to decrease the negative impacts. Because sharing is not evenly distributed, in future research an assessment will be made of how the sharing factor changes across regions and time.

Battery Cost. In a separate sensitivity, the cost of batteries was varied (Figure 12). Higher-cost batteries lead to a fleet with shorter-range vehicles and vice versa. These shifts cause the total battery capacity procured for the fleet to vary from the base solution by +68% for \$25/kWh batteries, and by −4% for \$250/kWh batteries. In other words, expensive batteries incentivize a reduction in the total purchase of batteries which can only be achieved by distributing them among shorter-range vehicles. The total fleet size also increases very slightly with higher battery costs (<1%); this was attributed to the increased need for some vehicles to charge during the afternoon rush. Conversely, at lower battery costs—less than or equal to the base cost of \$150/kWh—when the fleet mix includes longer-range vehicles, the need for charging at 4 p.m. vanishes.

The change in fleet composition also changes the composition of the charging infrastructure. There are three

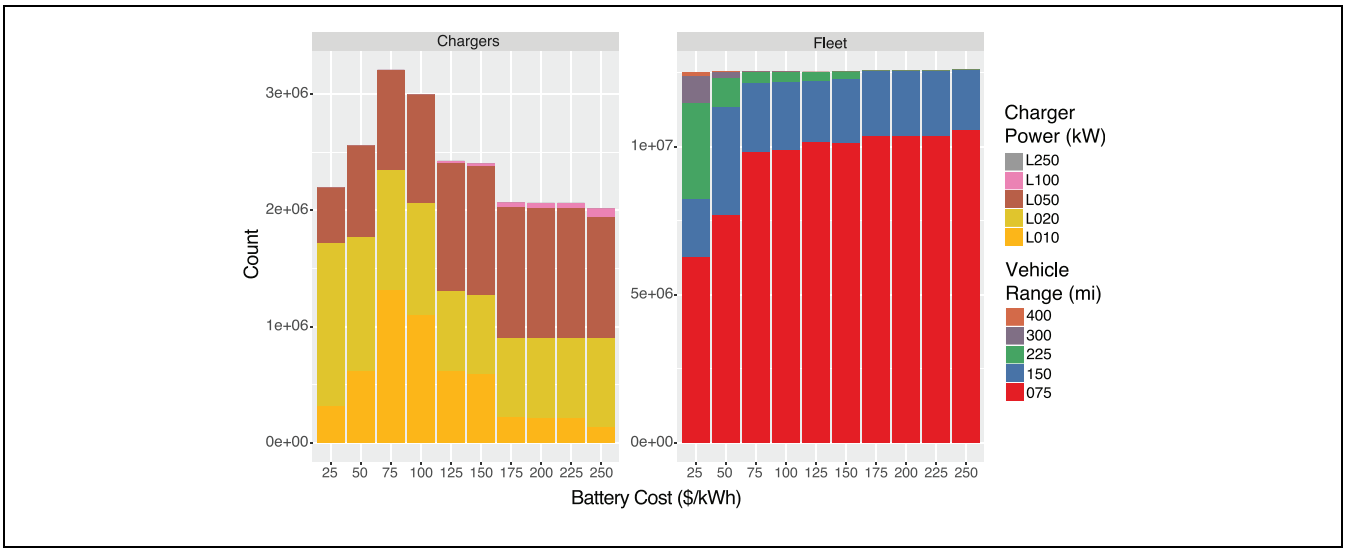

Figure 12. National charging infrastructure (*left*) and fleet composition (*right*) requirements for varying assumptions on battery cost (*x*-axis).

distinct trends, from $25-75/kWh, there is a substitution of 20kW for a combination of 50kW and 10kW chargers. From $75-150/kWh, the 50kW chargers increase at the expense of lower power charging. From $150-250/kWh, 100kW chargers enter the solution, composing 5–10% of the total power capacity of the infrastructure. In general, as the fleet shifts toward shorter-range vehicles, there is an increased reliance on higher-power chargers. Faster chargers allow lower-range vehicles to be quickly recharged and utilized in situations where a longer-range vehicle could have simply continued driving.

Price Shape. Finally, the impact of the shape of daily electricity price profile was explored. The scenarios are illustrated in Figure 4. The result of these different price scenarios on the aggregate charging profile is shown in Figure 13.

Across all scenarios, the charging profile in the first half of the day is almost identical but varies in instructive ways in the second half of the day, after the 4 p.m. mobility peak. In the flat pricing scenario, charging never returns to the maximum during the rest of the day, indicating that there is no binding constraint on when the vehicles charge in the absence of price variation. These two results support the general conclusion that across all scenarios, charging in the first half of the day is largely dispatched to supply mobility and charging in the second half of the day is largely dispatched to minimize energy costs. For the remaining price scenarios, the price-responsive charging follows common sense patterns, avoiding the highest cost hours in favor of the lowest cost.

Conclusion

We have formulated a quadratically constrained, quadratic programming problem designed to model the requirements of SAEVs at a national scale. The size of the SAEV fleet and the necessary charging infrastructure are treated as decision variables, allowing for heterogeneous vehicle ranges and charger levels. The model minimizes operational costs by choice of the timing of fleet recharging while requiring that mobility demand be served and energy conservation be maintained. Planning costs are simultaneously minimized by amortizing the cost of the fleet and charging infrastructure to a daily time period.

In the base scenario solution, it is found that all mobility in the U.S. currently served by 276 million personally owned vehicles could be served by 12.5 million SAEVs at a cost of $ 0.27/vehicle-mile. The energy requirements for this fleet would be 1142 GWh/day (8.5% of 2017 U.S. electricity demand) and the peak charging load 76.7 GW (11% of U.S. power peak).

The following tasks and model improvements remain for future research:

- Increase the number of days simulated to capture day to day and seasonal variability.
- Conduct further sensitivity analysis around regionally distinct pricing scenarios.
- Couple the model to a regional scale model of power generation; simultaneously minimize the cost of the mobility system with the cost of generating power.
- Add temporal overheads associated with charging and vehicle maintenance.

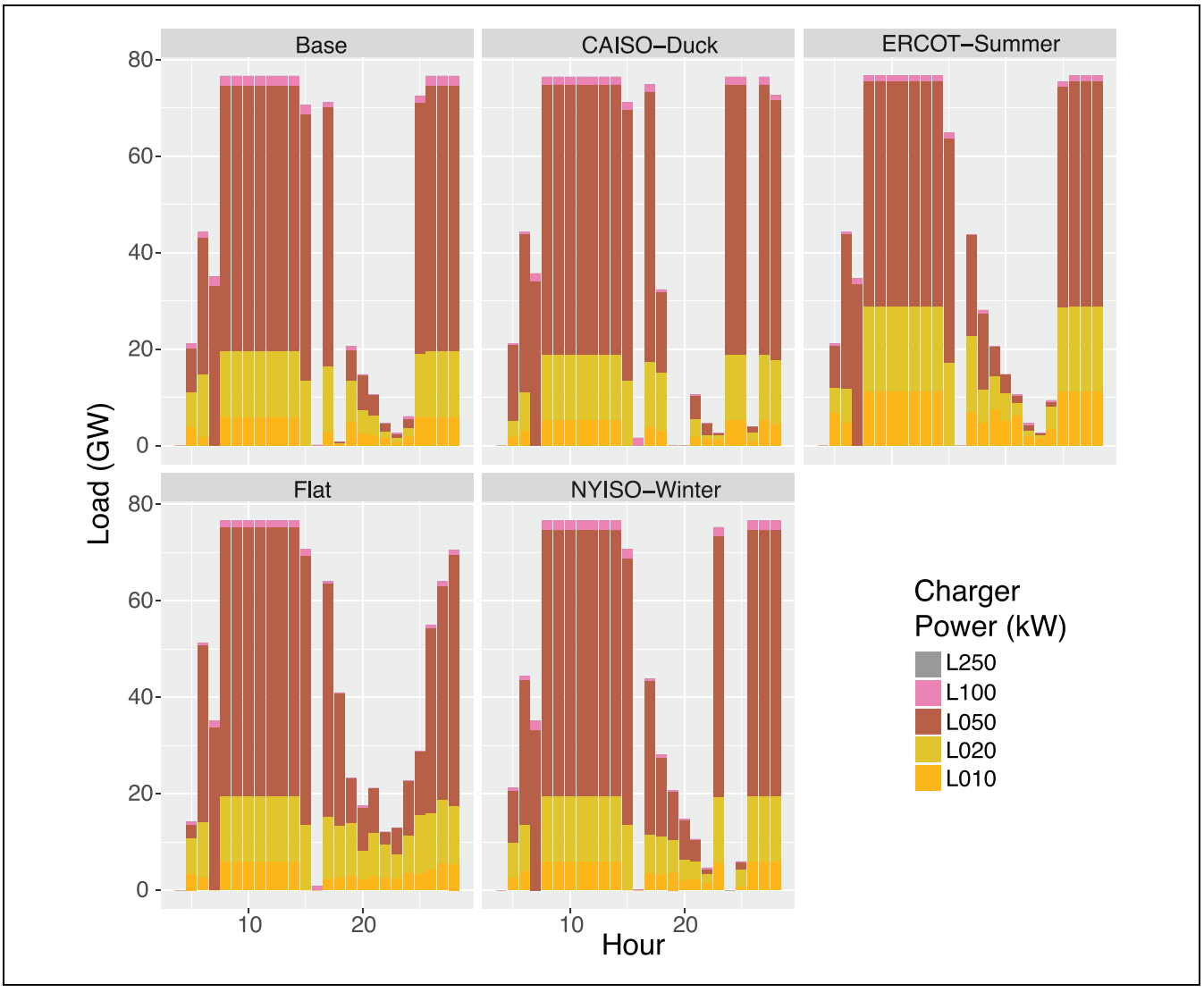

Figure 13. Resulting charging profile of national fleet by power capacity for various price assumptions.

- Model heterogeneous battery lifetimes based on simulated cycling.
- Include other forms of transportation electrification (personally owned and medium/heavy duty vehicles).
- Investigate heterogeneous sharing and include in the model.
- Investigate variability of urban form factor by trip distance and time of day.
- Investigate variation in the peak electricity demand over different days or seasons.

Acknowledgments

This report and the work described were sponsored by the U.S. Department of Energy (DOE) Vehicle Technologies Office (VTO) under the Vehicle Technologies Analysis Program. The following DOE Office of Energy Efficiency and Renewable Energy (EERE) managers played important roles in establishing the project concept, advancing implementation, and providing ongoing guidance: Rachael Nealer, Jake Ward, Kelly Fleming, and Heather Croteau. The authors also acknowledge Tom Stephens of Argonne National Laboratory, a collaborator and contributor to the inception of this analytical work. This work was funded by the U.S. Department of Energy Vehicle Technologies Office under Lawrence Berkeley National Laboratory Agreement No. #32048.

Author Contributions

The authors confirm contribution to the paper as follows: Study conception and design: CJRS, GSB, BFG, JBG, ATJ, ARG; Data collection: CJRS, GSB, BFG; Model development and implementation: CJRS (optimization model), GSB (GBB model); Analysis and interpretation of results: CJRS, GSB,

BFG, JBG, ATJ; Draft manuscript preparation: CJRS, GSB, BFG, JBG. All authors reviewed the results and approved the final version of the manuscript.

References

1. Hao, H., Y. Geng, and J. Sarkis. Carbon Footprint of Global Passenger Cars: Scenarios through 2050. *Energy*, Vol. 101, 2016, pp. 101–121.
2. United States Environmental Protection Agency. *Draft Inventory of U.S. Greenhouse Gas Emissions and Sinks: 1990-2016*, U.S. EPA, Washington, D. C., 2018.
3. Lah, O. Decarbonizing the Transportation Sector: Policy Options, Synergies, and Institutions to Deliver on a Low-carbon Stabilization Pathway. *Wiley Interdisciplinary Reviews: Energy and Environment*, Vol. 6, No. 6, 2017, p. e257.
4. Williams, J., A. DeBenedictis, R. Ghanadan, A. Mahone1, J. Moore, W. R. Morrow III, S. Price, and M. S. Torn. The Technology Path to Deep Greenhouse Gas Emissions Cuts by 2050: The Pivotal Role of Electricity. *Science*, Vol. 335, 2012, pp. 53–59.
5. Hawkins, T., O. Gausen, and A. Stromman. Environmental Impacts of Hybrid and Electric Vehicles—A Review. *The International Journal of Life Cycle Assessment*, Vol. 17, No. 8, 2012, pp. 997–1014.
6. Cai, H., and M. Xu. Greenhouse Gas Implications of Fleet Electrification Based on Big Data-Informed Individual Travel Patterns. *Environmental Science and Technology*, Vol. 47, No. 16, 2013, pp. 9035–9043.
7. Needell, Z., J. McNerney, M. Chang, and J. Trancik. Potential for Widespread Electrification of Personal Vehicle Travel in the United States. *Nature Energy*, Vol. 1, No. 9, 2016, p. 16112.
8. Saxena, S., J. MacDonald, and S. Moura. Charging Ahead on the Transition to Electric Vehicles with Standard Wall Outlets. *Applied Energy*, Vol. 120, 2015, pp. 720–728.
9. Office of California Governor Edmund G. Brown Jr. *Executive Order B-16-2012*, 2012.
10. Office of California Governor Edmund G. Brown Jr. *Governor Brown Delivers 2018 State of the State Address: California is Setting the Pace for America*, 25, 2018.
11. Force, Z. *Multi-State ZEV Action Plan: Accelerating the Adoption of Zero Emission Vehicles*, 2018.
12. Greenblatt, J., and S. Shaheen. Automated Vehicles and Mobility, On-Demand and Environmental Impacts. *Energy Reports*, Vol. 2, No. 3, 2015, pp. 74–81.
13. Martin, E., and S. Shaheen. Greenhouse Gas Emissions Impacts of Carsharing in North America. *IEEE Transactions on Intelligent Transportation Systems*, Vol. 12, No. 4, 2014, pp. 1074–1086.
14. Waymo: Phoenix Begins Testing Self-Driving Vans on Public Roads. *CBS News*, Nov. 7, 2018.
15. Sperling, D. *Three Revolution: Steering Automated, Shared, and Electric Vehicles to a Better Future*. Island Press, 2018.
16. Fulton, L. M. Three Revolutions in Urban Passenger Travel. *Joule*, 2018.
17. Greenblatt, J., and S. Saxena. Autonomous Taxis Could Greatly Reduce Greenhouse-Gas Emissions of US Light-Duty Vehicles. *Nature Climate Change*, 2015-09, pp. 860–865.
18. Green, E., S. Skerlos, and J. Winebrake. Increasing Electric Vehicle Policy Efficiency and Effectiveness by Reducing Mainstream Market Bias. *Energy Policy*, 2014, pp. 65–562.
19. King, C., W. Griggs, F. Wirth, K. Quinn, and R. Shorten. Alleviating a Form of Electric Vehicle Range Anxiety through On-Demand Vehicle Access. *International Journal of Control*, Vol. 88, No. 4, 2015, pp. 717–728.
20. Hawkins, A. J. *Waymo and Jaguar will Build Up to 20,000 Self-driving Electric SUVs*, 2018.
21. Stephens, T. S., J. Gonder, Y. Chen, Z. Lin, C. Liu, and D. Gohlke. *Estimated Bounds and Important Factors for Fuel Use and Consumer Costs of Connected and Automated Vehicles*. National Renewable Energy Lab, Golden, CO, 2016.
22. MacKenzie, D., Z. Wadud, and P. Leiby. A First Order Estimate of Energy Impacts of Automated Vehicles in the United States. Presented at the 93rd Annual Meeting of the Transportation Research Board, Washington, D.C., 2014.
23. Stocker, A., and S. Shaheen. *Shared Automated Vehicles: Review of Business Models*. Discussion Paper No. 2017-09. Transportation Sustainability Research Center, University of California, Berkeley, 2017.
24. Bosch, P. M., F. Becker, H. Becker, and K. W. Axhausen. Cost-based Analysis of Autonomous Mobility Services. *Transport Policy*, Vol. 64, 2018, pp. 76–91.
25. Fagnant, D. J., and K. Kockelman. Preparing a Nation for Autonomous Vehicles: Opportunities, Barriers and Policy Recommendations. *Transportation Research Part A: Policy and Practice*, Vol. 77, 2015, pp. 167–181.
26. Daziano, R. A., M. Sarrias, and B. Leard. Are Consumers Willing to Pay to Let Cars Drive for Them? Analyzing Response to Autonomous Vehicles. *Transportation Research Part C: Emerging Technologies*, Vol. 78, 2017, pp. 150–164.
27. Litman, T. *Autonomous Vehicle Implementation Predictions*. Victoria Transport Policy Institute, 2017.
28. Zhang, W., S. Guhathakurta, and E. B. Khalil. The Impact of Private Autonomous Vehicles on Vehicle Ownership and Unoccupied VMT Generation. *Transportation Research Part C: Emerging Technologies*, Vol. 90, 2018, pp. 156–165.
29. Chen, T. D., K. M. Kockelman, and J. P. Hanna. Operations of a Shared, Autonomous, Electric Vehicle fleet: Implications of Vehicle & Charging Infrastructure Decisions. *Transportation Research Part A: Policy and Practice*, Vol. 94, 2016, pp. 243–254.
30. Luk, J., H. Kim, R. Kleine, T. Wallington, and H. Maclean. Review of the Fuel Saving, Life Cycle GHG Emission, and Ownership Cost Impacts of Lightweighting Vehicles. *Environmental Science and Technology*, Vol. 51, No. 15, 2017, pp. 8215–8228.
31. Bauer, G. S., J. B. Greenblatt, and B. F. Gerke. Cost, Energy, and Environmental Impact of Automated Electric Taxi Fleets in Manhattan. *Environmental Science and Technology*, Vol. 52, No. 8, 2018, pp. 4920–4928.

32. Johnson, C., and J. Walker. *Peak Car Ownership: The Market Opportunity of Electric Automated Mobility Services*. Boulder, CO, 2016.
33. Franke, T., and J. F. Krems. Understanding Charging Behaviour of Electric Vehicle Users. *Transportation Research Part F: Traffic Psychology and Behaviour*, Vol. 21, 2013, pp. 75–89.
34. Franke, T., M. Gunther, M. Trantow, and J. F. Krems. Does This Range Suit Me? Range Satisfaction of Battery Electric Vehicle Users. *Applied Ergonomics*, Vol. 65, 2017, pp. 191–199.
35. Wolbertus, R., M. Kroesen, R. van den Hoed, and C. G. Chorus. Policy Effects on Charging Behaviour of Electric Vehicle Owners and On Purchase Intentions of Prospective Owners: Natural and Stated Choice Experiments. *Transportation Research Part D: Transport and Environment*, Vol. 62, 2018, pp. 283–297.
36. Melaina, M., M. Muratori, J. McLaren, and P. Schwabe. Investing in Alternative Fuel Infrastructure: Insights for California from Stakeholder Interviews: Preprint. *TRB*, Vol. Preprint, 2017, p. 16.
37. Smith, C., and J. Orenberg. *2015-2016 Investment Plan Update for the Alternative and Renewable Fuel and Vehicle Technology Program*, Docket Number: 14-ALT-01. California Energy Commission, Sacramento, CA, 2015.
38. John, J. S. *California Utilities Seek $1B to Build Out Electric Vehicle Infrastructure*, Greentech Media, MA, 2017.
39. America, E. *California ZEV Investment Plan: Cycle 1 -Electrify America*. Volkswagen, Group of America, 2017.
40. Reuters, Volkswagen to Install 2,800 U.S. Electric Vehicle Charging Stations. *Reuters*, 2017.
41. Nelson, J. H., and L. M. Wisland. *Achieving 50 Percent Renewable Electricity in California: The Role of Non-Fossil Flexibility in a Cleaner Electricity Grid*, Union of Concerned Scientists, Cambridge, MA, 2015.
42. Peter, A., J. Potter, M. A. Piette, P. Schwartz, M. A. Berger, L. N. Dunn, S. J. Smith, M. D. Sohn, A. Aghajanzadeh, S. Stensson, J. Szinai, T. Walter, L. McKenzie, L. Lavin, B. Schneiderman, A. Mileva, E. Cutter, A. Olson, J. Bode, A. Ciccone, and A. Jain. *Final Report on Phase 2 Results, 2015 California Demand Response Potential Study: Charting California's Demand Response Future*. Lawrence Berkeley National Laboratory, Energy and Environmental Economics, and Nexant, 2016.
43. Richardson, D. B. Electric Vehicles and The Electric Grid: A Review of Modeling Approaches, Impacts, and Renewable Energy Integration. *Renewable and Sustainable Energy Reviews*, Vol. 19, 2013, pp. 247–254.
44. Foley, A., B. Tyther, P. Calnan, and B. O. Gallachoir Impacts of Electric Vehicle Charging under Electricity Market Operations. *Applied Energy*, Vol. 101, 2013, pp. 93–102.
45. Sheppard, C., J. Szinai, N. Abhyankar, and A. Gopal. *Grid Impacts of Electric Vehicles and Managed Charging in California: Linking Agent-Based Electric Vehicle Charging with Power System Dispatch Models*. Lawrence Berkeley National Laboratory, 2018.
46. Lopes, J., F. Soares, and P. Almeida. Integration of Electric Vehicles in the Electric Power System. *Proceedings of the IEEE*, Vol. 99, 2011, pp. 168–183.
47. Tarroja, B. Assessing the Stationary Energy Storage Equivalency of Vehicle-to-Grid Charging Battery Electric Vehicles. *Energy*, Vol. 106, 2016, pp. 673–690.
48. Forrest, K. Charging a Renewable Future: The Impact of Electric Vehicle Charging Intelligence on Energy Storage Requirements to Meet Renewable Portfolio Standards. *Journal of Power Sources*, Vol. 336, 2016, pp. 63–74.
49. Coignard, J., S. Saxena, J. Greenblatt, and D. Wang. Clean Vehicles as an Enabler for a Clean Electricity Grid. *Environmental Research Letters*, 2018.
50. Short, W., and P. Denholm. A Preliminary Assessment of Plug-In Hybrid Electric Vehicles on Wind Energy Markets, National Renewable. National Renewable Energy Lab, Golden, CO, 2006.
51. Lund, H., and W. Kempton. Integration of Renewable Energy into the Transport and Electricity Sectors through V2G. *Energy Policy*, Vol. 36, 2008, pp. 3578–3587.
52. Juul, N., and P. Meibom. Road Transport and Power System Scenarios for Northern Europe in 2030. *Applied Energy*, Vol. 92, 2012, pp. 573–582.
53. Liu, W. Electric Vehicles and Large-Scale Integration of Wind Power—The Case of Inner Mongolia in China. *Applied Energy*, Vol. 104, 2013, pp. 445–456.
54. Borba, B., A. Szklo, and R. Schaeffer. Plug-In Hybrid Electric Vehicles as a Way to Maximize the Integration of Variable Renewable Energy in Power Systems: The Case of Wind Generation in Northeastern Brazil. *Energy*, Vol. 37, 2012, pp. 469–481.
55. Kempton, W., and J. Tomić. Vehicle-to-Grid Power Implementation: From Stabilizing the Grid to Supporting Large-scale Renewable Energy. *Journal of Power Sources*, Vol. 144, 2005, pp. 280–294.
56. Birnie, D. Solar-to-Vehicle (S2V) Systems for Powering Commuters of the Future. *Journal of Power Sources*, Vol. 186, 2009, pp. 539–542.
57. Neumann, H.-M., D. SchÃd'r, and F. Baumgartner. The Potential of Photovoltaic Carports to Cover the Energy Demand of Road Passenger Transport. *Progress in Photovoltaics: Research and Applications*, Vol. 20, 2012, pp. 639–649.
58. Gibson, T., and N. Kelly. Solar Photovoltaic Charging of Lithium-Ion Batteries. *Journal of Power Sources*, Vol. 195, 2010, pp. 3928–3932.
59. Chandra, M. System Design for a Solar Powered Electric Vehicle Charging Station for Workplaces. *Applied Energy*, Vol. 168, 2016, pp. 434–443.
60. Drude, L. Photovoltaics (PV) and Electric Vehicle-to-Grid (V2G) Strategies for Peak Demand Reduction in Urban Regions in Brazil in a Smart Grid Environment. *Renewable Energy*, Vol. 68, 2014, pp. 443–451.
61. Qi, Z. Integration of PV Power into Future Low-Carbon Smart Electricity Systems with EV and HP in Kansai Area, Japan, Renewable. *Energy*, Vol. 44, 2012, pp. 99–108.
62. Deng, C., N. Liang, J. Tan, and G. Wang. Multi-Objective Scheduling of Electric Vehicles in Smart Distribution Network. *Sustainability*, Vol. 8, No. 12, 2016, p. 1234.
63. Guo, Q., Y. Wang, H. Sun, Z. Li, S. Xin, and B. Zhang. Factor Analysis of the Aggregated Electric Vehicle Load Based on Data Mining. *Energies*, Vol. 5, No. 6, 2012, pp. 2053–2070.

64. Mullan, J., D. Harries, T. Braunl, and S. Whitely. Modelling the Impacts of Electric Vehicle Recharging on the Western Australian Electricity Supply System. *Energy Policy*, Vol. 39, No. 7, 2011, pp. 4349–4359.
65. Axsen, J., and K. S. Kurani. Anticipating Plug-in Hybrid Vehicle Energy Impacts in California: Constructing Consumer-informed Recharge Profiles. *Transportation Research Part D*, Vol. 15, No. 4, 2010, pp. 212–219.
66. Darabi, Z., and M. Ferdowsi. Aggregated Impact of Plug-in Hybrid Electric Vehicles on Electricity Demand Profile. *IEEE Transactions on Sustainable Energy*, Vol. 2, No. 4, 2011, pp. 501–508.
67. Wood, E., S. Raghavan, C. Rames, J. Eichman, and M. Melaina. *Regional Charging Infrastructure for Plug-In Electric Vehicles: A Case Study of Massachusetts*. National Renewable Energy Lab, Golden, CO, 2017.
68. Gerkensmeyer, C., M. C. Kintner-Meyer, and J. G. DeSteese. *Technical Challenges of Plug-In Hybrid Electric Vehicles and Impacts to the US Power System: Distribution System Analysis*. Pacific Northwest National Lab, 2010.
69. Fagnant, D., and K. Kockelman. The Travel and Environmental Implications of Shared Autonomous Vehicles, Using Agent-Based Model Scenarios. *Transportation Research Part C: Emerging Technologies*, Vol. 2014, No. 40, 2014, pp. 1–13.
70. Fagnant, D., K. Kockelman, and P. Bansal. *Operations of Shared Autonomous Vehicle Fleet for Austin*, 2015.
71. Chen, T. Management of a Shared, Autonomous, Electric Vehicle Fleet: Vehicle Choice, Charging. Infrastructure & Pricing Strategies. PhD dissertation. University of Texas, Austin, TX, 2015.
72. Bischoff, J., and M. Maciejewski, Agent-Based Simulation of Electric Taxicab Fleets. *Transportation Research* Procedia, Vol. 2014, No. 4, 2014, pp. 191–198.
73. Bischoff, J., and M. Maciejewski. Electric Taxis in Berlin - Analysis of the Feasibility of a Large-Scale Transition. In Tools of Transport Telematics. In *Communications in Computer and Information Science* (J. Mikulski, ed.), Springer, Cham, Vol. 531, 2015, pp. 343–351.
74. Loeb, B. Shared Autonomous Electric Vehicle (SAEV) Operations across the Austin, Texas Network with a Focus on Charging Infrastructure Decisions. *Transportation Research Part C Emerging Technologies*, Vol. 89, 2016, pp. 222–233.
75. U.S. Department of Transportation, Federal Highway Administration. *2017 National Household Travel Survey*, 2017.
76. *EIA -Electricity Data*, 2018.
77. National Renewable Energy Laboratory. *Utility Rate Database Open Energy Information*, 2018.

The Standing Committee on Transportation Energy (ADC70) peer-reviewed this paper (19-04914).